Available online at www.sciencedirect.com
SCIENCE DIRECT®
Thermochimica Acta 433 (2005) 98–104
thermochimica acta
www.elsevier.com/locate/tca

Thermal characterization of overmolded underfill materials for stacked chip scale packages

Yi He *

Assembly Materials Characterization Laboratory, Intel Corporation, CH5-232, 5000 W. Chandler Blvd., Chandler, AZ 85226-3699, USA

Received 16 November 2004; received in revised form 1 February 2005; accepted 14 February 2005
Available online 16 March 2005

Abstract

Stacked chip scale package (SCSP) is a new electronic packaging technology for non-CPU products, such as hand-held computing and communication devices. In this technology, one or more wire-bonded silicon chips are stacked on top of another flipped silicon chip, and an overmolded underfill encapsulant is used to both encapsulate and underfill the wire-bonded chip and the flip chip in a single process. In this paper, the cure behavior, thermal stability, filler content, and thermomechanical properties of five overmolded underfill materials have been studied using DSC, TGA, TMA, and DMA. Results showed that there is a strong correlation between thermomechanical properties and the filler content of the material. Based on measured thermomechanical properties, a "figure-of-merit" approach was used to estimate the thermal stress induced in the package upon cooling. Results showed that an OMUF material with a low T_g, low coefficient of thermal expansion (CTE), and low modulus can effectively reduce the package thermal stress. The reliability results are in good agreement with the predictions based on thermal stress estimation.

Keywords: Thermal characterization; Underfill materials; SCSP

1. Introduction

Flip chip technology, first invented by IBM more than 30 years ago [1], has been used for a long time in advanced electronic packaging [2–4]. In this technology, the active side of the silicon chip is placed toward the substrate by a variety of surface mount technologies [4]. Flip chip technology provides excellent electrical performance, high input/output density, and high interconnection speed. In addition, it offers good manufacturability and is highly reliable. In this technology, a liquid underfill encapsulant is used to fill the gap between the silicon chip and the substrate through a capillary flow process. When cured, the underfill encapsulant can serve multiple purposes: it reduces package stresses caused by mismatch in the coefficient of thermal expansion (CTE) between the silicon, the solder alloy, and the organic substrate; it protects the silicon chip from the external environment; and it also provides mechanical strength to the whole package. As a result, the solder joint reliability and package service life have been greatly improved [4].

As semiconductor devices become smaller and smaller with increased functionality, a new class of electronic package, called chip scale package (CSP), has emerged [5]. In this type of package, the package area is no more than 1.5 times the area of the silicon chip. CSP technology has been used to package non-CPU devices, such as flash memory chips used in hand-held computing and wireless communication devices. To accommodate the continuous trend of device miniaturization and increased functionality, a new extension of CSP technology, called stacked chip scale package (SCSP), has been developed [6]. In one configuration of SCSP, one or more wire-bonded silicon chips are stacked on top of a flip chip, as illustrated in Fig. 1. The advantage of SCSP is the shortened interconnect distance, which reduces signal delays and capacitance, leading to increased device speed

* Tel.: +1 480 5523154; fax: +1 480 5545241.
E-mail address: yi.he@intel.com.

0040-6031/$ – see front matter © 2005 Elsevier B.V. All rights reserved.
doi:10.1016/j.tca.2005.02.020

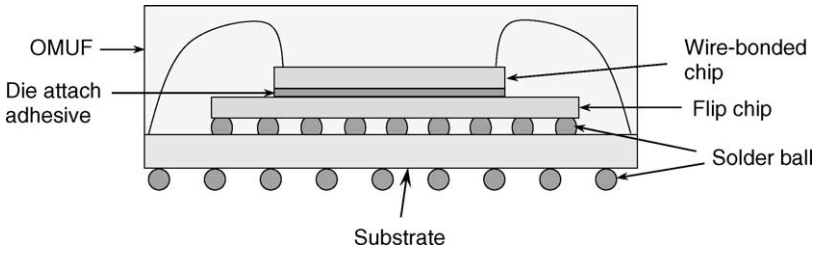

Fig. 1. Illustration of a stacked chip scale package encapsulated using an overmolded underfill material.

and reduced noise. Since the introduction of the first SCSP product in 1998 by Sharp Corp. in Japan to stack bare-die flash and SRAM chips for cell phones, many semiconductor companies have produced millions of SCSPs for wireless communication devices [7].

Traditionally, a capillary flow underfill material is dispensed between the flip chip and the substrate. This method poses several challenges for SCSP, such as slow underfill flow time, underfill voids, and high assembly cost. In addition, a molding compound is needed to encapsulate the stacked die, which will result in underfill-molding compound integration problems. An alternative method is to use transfer-molding technology in which an overmolded underfill (OMUF) is used as a one-step material solution to package (Fig. 1) [8,9]. The overmolded underfill technology offers the advantage of significant process simplification and cost reduction. Transfer-molding technology allows the use of higher filler content in the OMUF without creating flow problems that typically face the conventional capillary flow underfill materials. This increase in filler content lowers the CTE of the OMUF, which reduces the CTE mismatch between the silicon die and the OMUF, thereby leading to lower thermal stresses in the package. In addition, compared to capillary flow underfill materials, OMUF materials have a higher mechanical strength and moisture resistance, which will improve package reliability performance.

Because of its strategic function in the package, the material properties of the OMUF materials are very important. In this study, we investigated the material properties of five overmolded underfill materials for potential SCSP applications. In particular, the curing behavior of these materials was studied using DSC, the thermal stability and filler content were analyzed using TGA, and the thermomechanical properties of cured materials were investigated using TMA and DMA. The measured properties allow us to estimate the CTE mismatch-induced thermal stress in the package, which is very important for material selection.

2. Experimental

2.1. Material

OMUF materials from five different suppliers were characterized. These materials contain mainly epoxy, hardener, stress relief agent, coupling agent, silica filler, and carbon black pigment. The uncured materials were black pellets and were stored in a −40 °C freezer before use. For TMA and DMA studies, cured materials were used. The cured bulk samples were in the shape of circular disks or rectangular rods. They were transfer-molded at 175 °C (which lasts typically for 90 s) and post-mold cured at 180 °C for 2–4 h. DSC experiments on cured samples did not reveal any detectable residual heat of reaction, indicating that these materials were fully cured after post-mold cure. The main purpose of the post-mold cure is to provide enough time for the coupling agent to diffuse across the interfacial boundaries between the OMUF and the substrate or the silicon chip, thus improving the adhesion property of the OMUF. An added benefit is that it also provides an opportunity to relax the internal stress accumulated from the transfer-molding and the cure processes, which will reduce the package warpage.

2.2. DSC

The curing behavior of the OMUF materials was studied with a TA Instruments 2920 modulated DSC operated in standard mode. The DSC cell was purged with nitrogen at a rate of 30 cm^3/min. The sample was hermetically sealed in an aluminum DSC pan and was heated from 25 to 300 °C at 10 °C/min. The typical sample size was 20 mg. The DSC measurement, like all other experiments discussed below, was repeated three times for each material.

2.3. TGA

The thermal stability and the filler content of the OMUF materials were examined using a TA Instruments TGA 2950 Thermogravimetric Analyzer. All TGA measurements were conducted in an air atmosphere by heating the uncured OMUF samples from 25 to 600 °C at a heating rate of 10 °C/min, followed by holding the sample at 600 °C for 30 min. The air flow rate was about 70 cm^3/min. The typical sample size was 10–30 mg.

2.4. TMA

The linear coefficient of thermal expansion (CTE), α, of cured OMUF samples was measured using a Perkin-Elmer TMA7 thermomechanical analyzer in expansion mode. The

TMA sample stage was purged with nitrogen at a rate of 34 cm^3/min. TMA specimens were cut from the cured bulk sample with a low-speed diamond saw. The sample length was typically 4–5 mm, and the width and the thickness were about 2–3 mm. The TMA loading force was kept at 10 mN to minimize stress-induced sample deformation. During the TMA measurement, the specimen was heated from −50 to 300 °C at 10 °C/min. For each measurement, two heating ramps were used. The first heating scan was used to eliminate any possible internal stress and moisture in the OMUF generated during the curing and sample preparation process. During the second heating ramp, the CTE of the material can be determined. However, to minimize the stress effect, the CTE values were also determined using the cooling curves, as shall be discussed later.

2.5. DMA

Dynamic mechanical behavior of cured OMUF materials was measured using a Perkin-Elmer DMA7 dynamic mechanical analyzer operated under three-point bending geometry. The experiment was carried out from −40 to 300 °C at a heating rate of 5 °C/min. The sample length was 20 mm, the typical width was 2–3 mm, and the thickness was about 1.5 mm. During the measurement, the applied static force was kept at 120 mN, while the dynamic force was maintained at 100 mN. The dynamic frequency was 1 Hz.

3. Curing reaction

Fig. 2 plots the DSC curing curves of the five OMUF materials. The average curing onset and peak temperatures, as well as the total heat of the reaction, are summarized in Table 1. From Fig. 2 and Table 1, we can conclude that the OMUF materials from suppliers 2 through 5 have similar curing onset temperatures between 116 and 118 °C. OMUF1 has a slightly higher curing onset temperature at about 124 °C. All five OMUFs have similar curing peak temperatures in the range between 149 and 154 °C. Based on the DSC results shown in Fig. 2, it is clear that all of these materials can be fully cured after a short time at 175 °C, which is the recommended transfer-molding temperature.

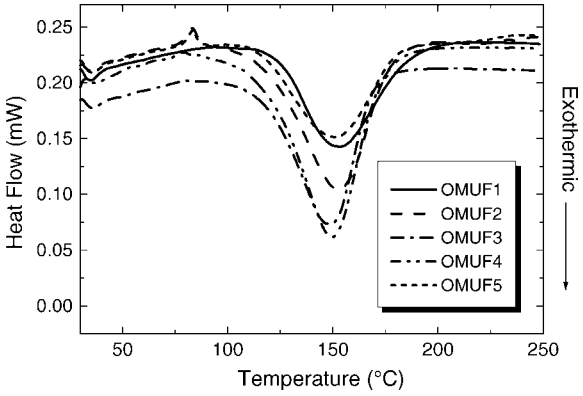

Fig. 2. DSC curves of five different OMUF materials determined at a heating rate of 10 °C/min.

4. Thermal stability and filler content

Thermal stability is a key material property for an OMUF. This is because after the package is assembled, it will be reflowed at high temperatures so that the solder balls on the substrate can be melted and attached to the motherboard to establish package-level interconnection. With the introduction of lead-free solder alloys in the electronic industry [10],

Table 1
General chemistry and material properties for the five OMUFs characterized by thermal analysis techniques

Material	OMUF1	OMUF2	OMUF3	OMUF4	OMUF5
Epoxy chemistry	Biphenyl	Multi-functional blend	Multi-functional/biphenyl	Multi-functional/biphenyl	Low molecular weight resin
Hardener	Phenol	Multi-functional phenol	Multi-functional blend	Multi-functional phenol	Phenol
Cure onset (°C)	123.8	117.8	117.8	116.4	116.6
Cure peak (°C)	154.1	153.2	149.3	149.6	151.3
ΔH (J/g)	21.78	28.9	25.3	36.8	19.8
Weight loss @ 175 °C (wt.%)	0.29	0.41	0.24	0.16	0.20
Weight loss @ 260 °C (wt.%)	0.38	0.64	0.30	0.23	0.30
Degradation onset (°C)	362	360	347	368	365
Filler content (wt.%)	88.96	80.79	86.73	84.66	86.35
α_1 (10^{-6} K^{-1}) (0–50 °C)	7.8	13.5	8.1	10.4	9.7
α_2 (10^{-6} K^{-1}) (200–250 °C)	46.1	77.4	48.6	41.3	45.7
TMA T_g (°C)	97.4	141.0	140.9	144.4	110.8
E' @ 25 °C (GPa)	23.1	11.4	19.0	19.8	20.5
E' @ 175 °C (GPa)	0.76	0.85	0.77	1.1	0.73
E' onset (°C)	57.3	126.9	120.6	123.4	97.0
E'' peak (°C)	73.5	145.9	134.3	137.8	109.4
T_g (tan δ peak, °C)	97.8	167.6	148.5	154.5	123.3

CTE1 (α_1), CTE2 (α_2), and the TMA T_g were determined from the cooling scan. All values are based on the average of three individual measurements.

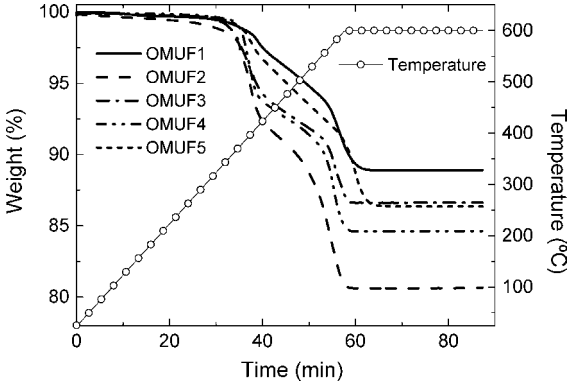

Fig. 3. TGA weight loss curves for five different OMUF materials measured between 25 and 600 °C at 10 °C/min.

the reflow temperature can be as high as 260 °C. Thus, an OMUF material has to be able to withstand that temperature without significant degradation. Fig. 3 shows the TGA curves of the five OMUFs. At 175 °C, which is the transfer-molding temperature, OMUF4 has the lowest weight loss of 0.16%, while OMUF2 has the highest weight loss, which is 0.26%. At 260 °C, the lowest weight loss is 0.23% for OMUF4 and the highest is 0.64% for OMUF2. All five OMUFs have degradation onset temperatures greater than 340 °C, which is considerably higher than the reflow temperature. In addition, the typical time spent at the reflow temperature was only 30 s. Thus all five OMUFs are considered stable at 260 °C without substantial degradation. Upon heating to 600 °C, the solid content, which is essentially inorganic fillers, is easily determined. The filler content has the following order: OMUF1 > OMUF3 ≈ OMUF5 > OMUF4 > OMUF2.

As shown in Table 1, OMUF1 has the highest filler content of nearly 89 wt.%, while OMUF2 has the lowest filler content of ∼81 wt.%. As we shall see later, a small difference (a few percent) in filler content can have an important impact on thermomechanical properties of these materials.

5. Thermal expansion

Fig. 4(a) plots the relative change in sample length ($\Delta L/L_0$) as a function of temperature during the second heating scan. It is interesting to note that OMUF1 and OMUF2 showed an abnormal swelling behavior near T_g, which is attributed to the release of stresses developed on cooling [11]. To minimize the stress effect on the thermal expansion behavior, we used the cooling curves to calculate the α values, as shown in Fig. 4(b), in which $\Delta L/L_0$ versus T curves were plotted from the cooling ramp of the experiment. Based on Fig. 4(b), α_1, which is the CTE below the glass transition temperature, was calculated for each material, as summarized in Table 1. A range of 0–50 °C was used for the α_1 calculation for all materials. The TMA results indicated that OMUF1 has the lowest α_1 of $7.8 \times 10^{-6}\,K^{-1}$; this is closely followed by OMUF3, which has an α_1 of $8.1 \times 10^{-6}\,K^{-1}$. OMUF2

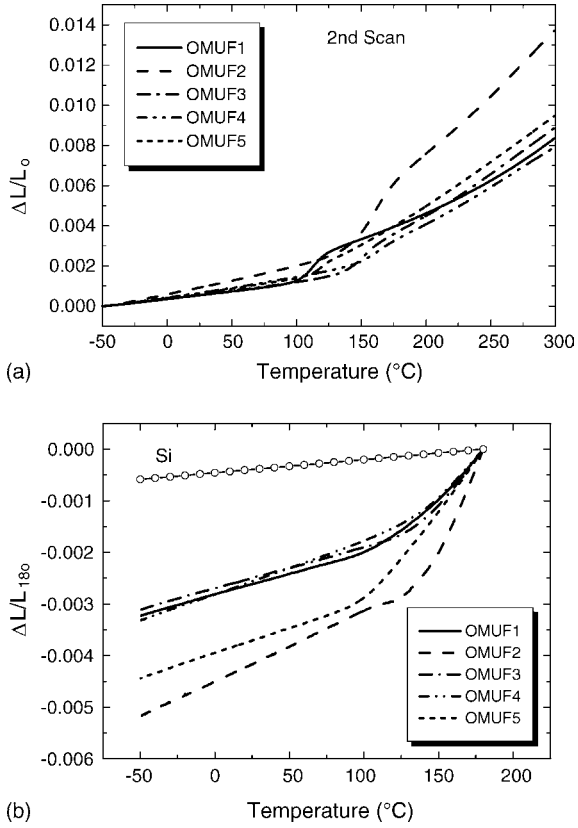

Fig. 4. (a) Relative change in sample length as a function of temperature for five OMUF materials determined from the second heating scan. The original length L_0 is taken as the sample length at −50 °C (after the first heating and the cooling ramps). For OMUF1 and OMUF2, the abnormal expansion behavior near T_g is attributed to the release of stresses developed on cooling. (b) Relative contraction in sample length determined from the cooling experiment. The reference temperature was taken as 180 °C, which is the post-mold cure temperature. L_{180} is the sample length at 180 °C. The stress effect on thermal expansion/contraction is significantly reduced. The relative contraction for silicon was also plotted.

has the highest α_1 of $13.5 \times 10^{-6}\,K^{-1}$. For OMUF4 and OMUF5, $\alpha_1 = 10.4 \times 10^{-6}$ and $9.7 \times 10^{-6}\,K^{-1}$, respectively. Overall, α_1 has the following order: OMUF1 ≤ OMUF3 < OMUF5 < OMUF4 < OMUF2, which reflects the effect of the inorganic filler content on the thermal expansion: a higher filler content leads to a lower CTE, and vice versa. At $T > T_g$, α_2 was calculated between 200 and 250 °C, and the results were listed in Table 1. Because OMUF1, OMUF3, OMUF4, and OMUF5 have very similar filler content, they have similar CTE values at either below or above T_g, as expected.

The glass transition temperatures obtained from TMA experiments were listed in Table 1. These values were obtained during the cooling experiments and were determined from the inflection point of the TMA traces. From the TMA results, OMUF1 has the lowest T_g of approximately 97.4 °C, and OMUF4 has the highest T_g of 144.4 °C. For OMUF1, the determined TMA T_g is not considered very accurate because for this material, the T_g transition is quite broad, as we shall see from the DMA data.

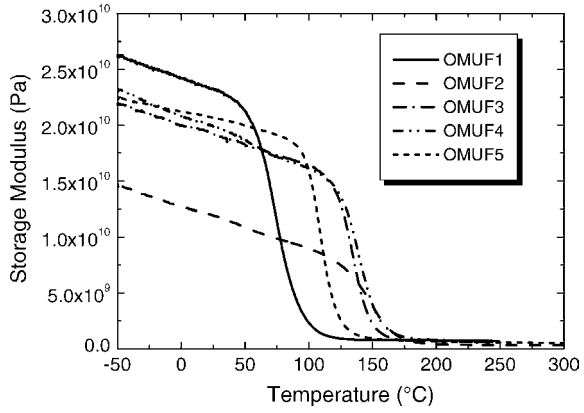

Fig. 5. Storage modulus as a function of temperature for five different OMUFs.

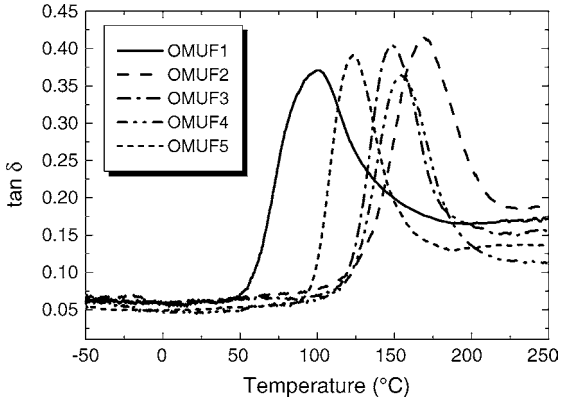

Fig. 6. Loss tangent as a function of temperature for five OMUF materials.

6. Dynamic mechanical properties

Fig. 5 plots the storage modulus, E', of the five cured OMUF materials as a function of temperature at a dynamic frequency of 1.0 Hz. It is clear that at room temperature, OMUF1 has the highest storage modulus, while OMUF2 has the lowest storage modulus. Again, these results are consistent with the TGA results on filler content. At room temperature, the storage moduli decrease in magnitude in the following order: OMUF1 > OMUF5 ≥ OMUF4 ≥ OMUF3 > OMUF2.

OMUF5, OMUF4, and OMUF3 have similar room temperature storage moduli, which again reflects the fact that these three materials contain similar amounts of filler (within ~2 wt.%). At 25 °C, E' is 23.1 GPa for OMUF1 and 11.4 GPa for OMUF2. For OMUF3 through OMUF5, E' = 19.0, 19.8, and 20.5 GPa at 25 °C, respectively, as listed in Table 1.

At the curing temperature (175 °C), the storage moduli of all OMUF materials were significantly lower, as indicated by Fig. 5 and Table 1. The onset temperatures for the reduction of E' due to the glass transition were also listed in Table 1. OMUF1 has the lowest E' onset temperature of 57.3 °C; and OMUF5 has the next lowest (97 °C). The other three materials have similar E' onset temperatures between 120 and 130 °C.

Fig. 6 plots the loss tangent curves of these materials. On average, OMUF1 has the lowest tan δ peak temperature of 97.8 °C, and OMUF2 has the highest tan δ peak temperature of 167.6 °C. The tan δ peak temperatures exhibited the following order: OMUF1 < OMUF5 < OMUF3 < OMUF4 < OMUF2. This is similar to the T_g trend determined by TMA.

7. Thermal stress estimation

During the transfer-molding process, the OMUF materials were cured in the mold at 175 °C for approximately 90–120 s before they were post-mold cured at 180 °C for 2–4 h. Once the stacked chip scale package starts to cool, stresses can develop due to cure shrinkage of the OMUF and the CTE mismatch between the silicon chips and the OMUF [12]. Typically, stress induced by CTE mismatch makes a much bigger contribution to the overall package stress. Therefore, we will ignore the stress due to cure shrinkage and only consider the CTE mismatch-induced thermal stress.

To further simplify the stress analysis, we adapt the approach used in Ref. [12] and consider only the interaction between the OMUF and the silicon chips. In this case, a "figure of merit" estimation of thermal stress developed in the electronic package during cooling can be expressed as [12]:

$$\sigma(T) = \int_{T_{\text{anch}}}^{T} \frac{\alpha - \alpha_s}{\frac{1}{E(T)} + \frac{A}{E_s}} \, dT, \tag{1}$$

where σ is the induced thermal stress; T_{anch} the "anchoring temperature", which is the smallest of the T_g, the cure temperature, and the post-cure temperature. Thus, $T_{\text{anch}} = T_g$. α and $E(T)$ are the CTE and the storage modulus of the OMUF, respectively. At $T < T_g$, α is nearly independent of temperature. α_s is the CTE of silicon, which is $2.55 \times 10^{-6}\,K^{-1}$ at room temperature [13,14]; E_s is the Young's modulus of silicon, which is 107 GPa, see for example [15], and A is a geometric factor on the order of unity. Since E_s is much larger than $E(T)$, Eq. (1) can be simplified as

$$\sigma(T) \approx \int_{T_{\text{anch}}}^{T} (\alpha - \alpha_s) E(T) \, dT. \tag{2}$$

In our calculation, T_{anch} was changed to $T_{\text{post-cure}}$ (180 °C) in Eq. (2) so that $\sigma(T)$ will not be underestimated. This is because these OMUF materials are highly filled, and their E' will only decrease by a factor of 10–30 across the T_g transition, while for an unfilled polymer material, it is quite common to see a 1000-fold reduction in E' across the T_g transition.

Based on Eq. (2) and the measured thermomechanical properties of the OMUF, thermal stress can be estimated numerically for these five materials. Fig. 7 plots the thermal stress developed upon cooling as a function of temperature in the electronic package using the above approach. Upon cool-

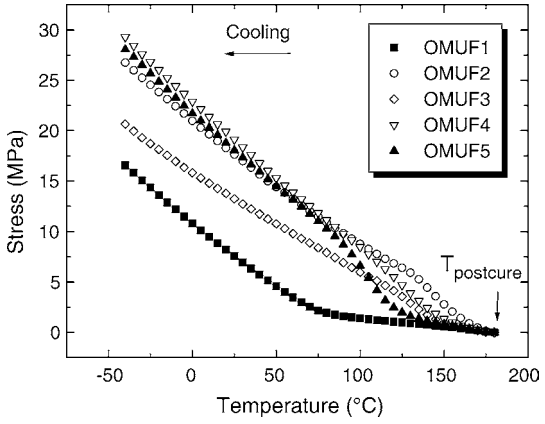

Fig. 7. Estimated thermal stress development in the electronic package upon cooling the OMUF from $T_{post\text{-}cure}$, which is the post-mold cure temperature (180 °C). CTE values obtained from the cooling experiments were used for this calculation.

ing to below the T_g of an OMUF material, thermal stress starts to increase significantly, as expected. OMUF1, which has the lowest T_g (based on both TMA and DMA results), the lowest CTE, and the highest E' at room temperature, has the lowest thermal stress at low temperatures. At 25 °C, the developed thermal stress is estimated to be 7.58 MPa. The remarkable behavior of OMUF1 demonstrated that low CTE combined with low T_g can reduce the thermal stress very effectively. OMUF3, on the other hand, has a relatively high T_g, but it also has the second lowest CTE and E' at room temperature. The combined effect is that OMUF3 has the second lowest stress at low temperatures (13.24 MPa at 25 °C), as shown in Fig. 7. Calculation also revealed that OMUF2, OMUF4, and OMUF5 have similarly high thermal stresses. OMUF2, the material with the highest CTE, the highest T_g (based on DMA results), and the lowest E' at 25 °C, induces a relatively high thermal stress.

The behavior of OMUF5 is interesting. This material has the second lowest T_g, but it also has the second highest E' at room temperature. As one can see from Fig. 7, between $T_{post\text{-}cure}$ and 105 °C (which is slightly below its T_g based on TMA measurement), OMUF5 has the second lowest thermal stress, which is only higher than that of OMUF1. As the temperature decreases to below 105 °C, the stress in OMUF5 begins to increase rather rapidly, which is mainly caused by the rapid increase in its storage modulus. In fact, the difference between the TMA T_g and the E' onset temperature is the smallest for OMUF5 (13.8 °C). Thus, when the temperature decreases from $T_{post\text{-}cure}$ to T_g, the CTE of OMUF5 decreases but it follows by a quick increase in E', which leads to a rapid increase in package thermal stress. On the other hand, the difference between the TMA T_g and the E' onset temperature is the biggest for OMUF1 (40.1 °C). Therefore, for OMUF1, when the temperature decreases from $T_{post\text{-}cure}$ to the TMA T_g, its CTE decreases rapidly and at the same time, its E' remains small for an appreciate amount of temperature range before it starts to increase. This is another factor which contributes to the small thermal stress in packages encapsulated with OMUF1.

Although both CTE and modulus are important for stress reduction, lowering the CTE is, in many cases, more effective in minimizing the package stress than lowering the modulus. If the CTE of the OMUF matches that of silicon, theoretically, the thermal stress can be reduced to zero regardless the storage modulus of the OMUF material. Thus, based on material properties and thermal stress analysis, OMUF1 is the preferred candidate for SCSP, and OMUF2, OMUF4, and OMUF5, having the similarly high thermal stress at $T < T_g$, will have a higher risk of generating cracks or delaminations within the packages during reliability tests. Reliability results on assembly units built with the five OMUFs revealed that this is indeed the case: SCSPs built with OMUF2 were much more susceptible to interfacial delamination, which is most likely due to its high moisture absorption and high thermal stress in the package induced upon cooling. On the other hand, test coupons built with OMUF1 showed the best reliability performance [16]. Therefore, results from reliability tests are in general agreement with the thermal stress analysis based on the thermomechanical properties of the OMUFs.

It should also be pointed out that the above estimation of package thermal stress is only a figure of merit approach. A detailed calculation of package stress distribution is certainly much more involved, especially when it involves more than one silicon chip. Finite element analysis is needed to accurately model the package stress. However, accurate thermomechanical properties for the OMUF material are essential for such a modeling task.

8. Conclusions

DSC, TGA, TMA, and DMA techniques have been used to characterize five overmolded underfill materials used to package stacked chip scale packages for non-CPU applications. Results suggested that the thermomechanical properties of these materials are correlated with their inorganic filler content. Material with a higher filler content leads to a lower CTE and a higher storage modulus at $T < T_g$, and vice versa.

Based on measured thermomechanical properties, a figure of merit approach was used to estimate the thermal stress induced in the package upon cooling from the post-mold cure temperature. Calculations revealed that OMUF1 should have the lowest thermal stress (7.58 MPa) at room temperature, because of its low T_g and low CTE at $T < T_g$. On the other hand, OMUF4 should have the highest thermal stress, which is 19.11 MPa at 25 °C. These results suggest that the CTE, the storage modulus, and the T_g of an OMUF material can all impact package thermal stress. This work also demonstrated that thermal characterization of material properties can provide a quick prediction of package reliability performance, which is important for material selection.

Acknowledgements

I would like to thank Alan Overson, Stacy Nakamura, Denise Crouch and Fred Cardona for experimental assistance, and Drs. Tom Miller and John Briscoe for carefully reviewing the manuscript. I also want to thank Dr. Rahul Manepalli for discussions on general chemistry of the materials used in this work.

References

[1] E. Davis, W. Harding, R. Schwartz, J. Corning, IBM J. Res. Dev. (April) (1964) 102.
[2] D.R. Halk, Surf. Mount Technol. (September) (1997) 54.
[3] D.P. Schnorr, in: C.A. Harper (Ed.), Electronic Packaging and Interconnection Handbook, 2nd ed., McGraw-Hill, New York, 1997, Chapter 10.
[4] J.H. Lau (Ed.), Flip Chip Technologies, McGraw-Hill, New York, 1995.
[5] J.H. Lau, S.W.R. Lee, Chip Scale Package, McGraw-Hill, New York, 1999.
[6] V. LeBonheur, T. Sterrett, F. Pon, T.T. Chen, R. Manepalli, Intel Assembly Test Technol. J. 4 (2001) 278.
[7] H. Goldstein, IEEE Spectrum (August) (2001) 46.
[8] P.O. Weber, Chip package with molded underfill, US Patent 6,038,136 (March 14, 2000);
P.O. Weber, Chip package with molded underfill, US Patent 6,324,069 (November 27, 2001).
[9] F. Liu, Y.P. Wang, K. Chai, T.D. Her, Proceedings of the 2001 IEEE Electronic Component Technology Conference, Orlando, FL, 2001, pp. 285–292.
[10] K. Suganuma, Curr. Opin. Sol. State Mater. Sci. 5 (2001) 55.
[11] R.B. Prime, in: E.A. Turi (Ed.), Thermal Characterization of Polymeric Materials, vol. 2, 2nd ed., Academic Press, San Diego, CA, 1997, Chapter 6, pp. 1445–1462.
[12] H.E. Bair, D.J. Boyle, J.T. Ryan, C.R. Taylor, S.C. Tighe, D.L. Crouthamel, Polym. Eng. Sci. 30 (1990) 609.
[13] C.A. Swenson, R.B. Roberts, G.K. White, in: G.K. White, M.L. Minges (Eds.), Thermophysical Properties of Some Key Solids, Oxford Pergamon Press, CODATA Bulletin 59, 1985, Chapter 4.
[14] G.K. White, Thermochim. Acta 218 (1993) 83.
[15] M.F. Ashby, D.R.H. Jones, Engineering Materials, vol. 1, Pergamon Press, Inc., New York, 1980, p. 31.
[16] C.K. Chee, T. Sterrett, V. LeBonheur, L. DeCesare, Y. He, in: J. Pang, A. Lu, S. Wong (Eds.), Proceedings of the GlobalTRONICS Technology Conference 2002, Singapore, September 3–5, 2002, pp. 47–54 [In this publication, MUF A is OMUF2; MUF B is OMUF5, MUF C is OMUF3, MUF D is OMUF4, and MUF E is OMUF1].